Photochemistry and Photobiology, 2020, 96: 883–889

Research Article

First Report on Photodynamic Inactivation of Archaea Including a Novel Method for High-Throughput Reduction Measurement

Daniel B. Eckl[1]*, Harald Huber[1] and Wolfgang Bäumler[2]

[1]Department of Microbiology, University of Regensburg, Regensburg, Germany
[2]Department of Dermatology, University Hospital Regensburg, Regensburg, Germany

Received 21 November 2019, accepted 16 December 2019, DOI: 10.1111/php.13229

ABSTRACT

Archaea are considered third, independent domain of living organisms besides eukaryotic and bacterial cells. To date, no report is available of photodynamic inactivation (PDI) of any archaeal cells. Two commercially available photosensitizers (SAPYR and TMPyP) were used to investigate photodynamic inactivation of *Halobacterium salinarum*. In addition, a novel high-throughput method was tested to evaluate microbial reduction *in vitro*. Due to the high salt content of the culture medium, the physical and chemical properties of photosensitizers were analyzed *via* spectroscopy and fluorescence-based DPBF assays. Attachment or uptake of photosensitizers to or in archaeal cells was investigated. The photodynamic inactivation of *Halobacterium salinarum* was evaluated *via* growth curve method allowing a high throughput of samples. The presented results indicate that the photodynamic mechanisms are working even in high salt environments. Either photosensitizer inactivated the archaeal cells with a reduction of 99.9% at least. The growth curves provided a fast and precise measurement of cell viability. The results show for the first time that PDI can kill not only bacterial cells but also robust archaea. The novel method for generating high-throughput growth curves provides benefits for future research regarding antimicrobial substances in general.

INTRODUCTION

At the very beginning of the 20th century, Oskar Raab and Hermann von Tappeiner discovered that *Paramecium* cells can be inactivated by simultaneous application of light and acridine dyes by a process called photodynamic mechanism (1–3). Now, it is well known that light is absorbed by such a photosensitizer molecule, which thereby generates reactive oxygen species (ROS). These ROS can destroy cells *via* oxidation of various cellular structures. Meanwhile, the photodynamic mechanism found its way into different medical fields termed photodynamic therapy of tumors (PDT) (4).

Another promising application of the photodynamic mechanism is PDI of microorganisms that has been proven efficient against viruses, bacteria and fungi. In PDI, a cationic photosensitizer is usually attached to the surface or taken up by the cell and ROS kill the cells or viruses *via* oxidative mechanisms (5). A variety of molecules were successfully tested as photosensitizers to be used in PDI like porphyrins, phthalocyanines, phenalenones, phenothiazines or flavins (5).

Photodynamic inactivation (PDI) is efficient in killing bacteria regardless their types or resistances to antibiotic substances (6,7). The photodynamic inactivation of antibiotic-resistant bacteria like methicillin-resistant *Staphylococcus aureus* (MRSA) was successfully shown on human skin *ex vivo* (8). When immobilizing photosensitizers as antimicrobial coating, a clinical study provided evidence that generated singlet oxygen can kill bacteria on near-patient surfaces (9). PDI was also successfully applied to inactivate different viruses (10–15). Also, fungi (16–20) can be killed with ease with different photosensitizers. Furthermore, photodynamic inactivation is capable of efficiently treating certain protozoa (21).

Thus, PDI can be applied to various pathogenic and non-pathogenic organisms spanning nearly all parts of known living matter. However, the scientific literature remains without any prove that this principle applies to archaea. This might be explained by the fact that there are no discrete pathogens within the archaea so far. However, scientists start to understand the importance of a healthy human microbiome that also contains archaea (22–24) although archaea are typically found in various extreme environments such as black smokers or hydrothermal vents. These organisms are called hyperthermophiles with optimal growth temperatures above 80°C. Some archaea have also been reported to be extremely tolerant to ionizing radiation such as the anaerobic Euryarchaeon *Thermococcus gammatolerans* (25). *Picrophilus oshimae* on the other hand is an organism that was isolated from a solfataric field in Hokkaido, Japan, that naturally has a pH of 2.2 and is therefore considered an acidophilic organism (26). Recently, archaeal signatures have been discovered on board the international space station that is the latest prove for archaea in artificial, human-inhabited environments (27).

Since PDI requires oxygen to generate ROS, such research in archaea is hampered since the majority of these organisms is considered anaerobic. Aerobic archaea usually require pH values at which photosensitizers are chemically destroyed (28).

Therefore, in this study the extremely halophilic organism *Halobacterium salinarum* (29), which grows aerobically at neutral pH values was investigated. Cells of the genus *Halobacterium* are rods or disk-shaped cells that stain Gram-negative and

Corresponding author email: daniel.eckl@ur.de (Daniel B. Eckl)

often contain gas vacuoles (30). The present study shows PDI of an Archaeum (*Halobacterium salinarum*) for the first time. Another goal of this study was the application of growth curves in order to evaluate the logarithmic reduction of viable cells like archaea. The application of growth curves allows a much higher throughput of samples compared to other methods such as pour plate, spread plate or drop plate methods (31,32).

MATERIALS AND METHODS

Photosensitizers. The Photosensitizer TMPyP was purchased from Sigma-Aldrich with a minimum dye content of 97%, while SAPYR, an exclusively singlet oxygen producing photosensitizer, was purchased from TriOptoTec GmbH, with a minimum dye content of 97%. Photosensitizer solutions were prepared in adequate concentrations of 2, 10, 20, 50 and 100 µmol L^{-1} in sterile sodium chloride solution (10% w/v).

Organism and cultivation. For inactivation, *Halobacterium salinarum*^{T} DSM 3754 was used. It was cultivated at 37°C for 48 h in a modified *Halobacterium* medium containing per liter 5 g yeast extract (Becton, Dickinson and Company, Sparks), 5 g casamino acids (Becton, Dickinson and Company), 1 g sodium glutamate (Merck KGaA, Darmstadt, Germany), 2 g potassium chloride (Carl Roth GmbH+Co. KG, Karlsruhe, Germany), 3 g sodium tetra citrate (Merck KGaA), 20 g magnesium sulfate heptahydrate (Merck KGaA) and 200 g sodium chloride (Carl Roth GmbH+Co. KG). Besides the organic compounds, all substances were provided in analytic grade. The medium was autoclaved at 121°C for 20 min in 50 mL Erlenmeyer flasks containing 20 mL medium.

Cell preparation. Cells were harvested *via* centrifugation of 10 mL medium transferred into sterile 15 mL reaction tubes. Centrifugation took place for 7 min at 4500 ***g***. The supernatant was discarded, and the pellet was suspended in 5 mL of sterile sodium chloride solution (10% w/v). These steps were repeated thrice in order to remove remaining culture medium. After harvesting, the optical density measured at 600 nm of the cells was adjusted to 0.6.

Photodynamic inactivation. The assays were conducted in 96-well plates. Column 1 of the plate contained 25 µL of archaeal cells with 25 µL of sodium chloride solution (10% w/v). Next five columns contained TMPyP as a photosensitizer in ascending concentration, namely 1, 5, 10, 25 and 50 µmol L^{-1} and 25 µL of archaeal cells. Columns 7–12 were prepared accordingly with SAPYR. Experiments were conducted at low ambient light conditions as described elsewhere (33). The assays were illuminated beneath a commercial blue light source (blue_v, Waldmann GmbH, Villingen-Schweningen, Germany) with a radiant exposure of 10.8 J cm^{-2}. Additionally to the illuminated sample, a dark control was treated in the same manner without irradiation for dye concentrations of 0 and 50 µmol L^{-1}. After illumination, 20 µL of the cell suspension were immediately transferred into 180 µL of prewarmed (37°C) culture medium in 96-well plates. Twelve wells of the well plate contained medium without cells and served as blank control. These so prepared well plates were placed in a spectral photometer (CLARIOStar, BMG LABTECH GmbH, Ortenberg, Germany). Internal incubator was set to 37°C, while the internal shaker was turned on every 5 min shaking at 200 rpm for 30 s. After every 5 min, the spectral photometer measured the optical density at 600 nm of all wells. In total, the measurement was carried out for 2245 min with an additional last measurement carried out at 4115 min in order to increase the limit of detection to around 3 orders of magnitude. As each experiment was performed in triplicates, mean values of the optical density values were calculated and plotted *via* SigmaPlot against the incubation time.

Calculation of microbial reduction. The method used in this report for calculation of the microbial reduction was performed in accordance with another report in a modified manner (34). Therefore, doubling time of the archaeal cells was calculated as t_D between an optical density of 0.1 and 0.2 in early exponential growth phase. The doubling times were calculated for the untreated control. The time difference in reaching the optical density of 600 nm of 0.1 of the control and illuminated cells was calculated and is further on called t. The logarithmic reduction shortly called ρ was subsequently calculated as described in the formula below.

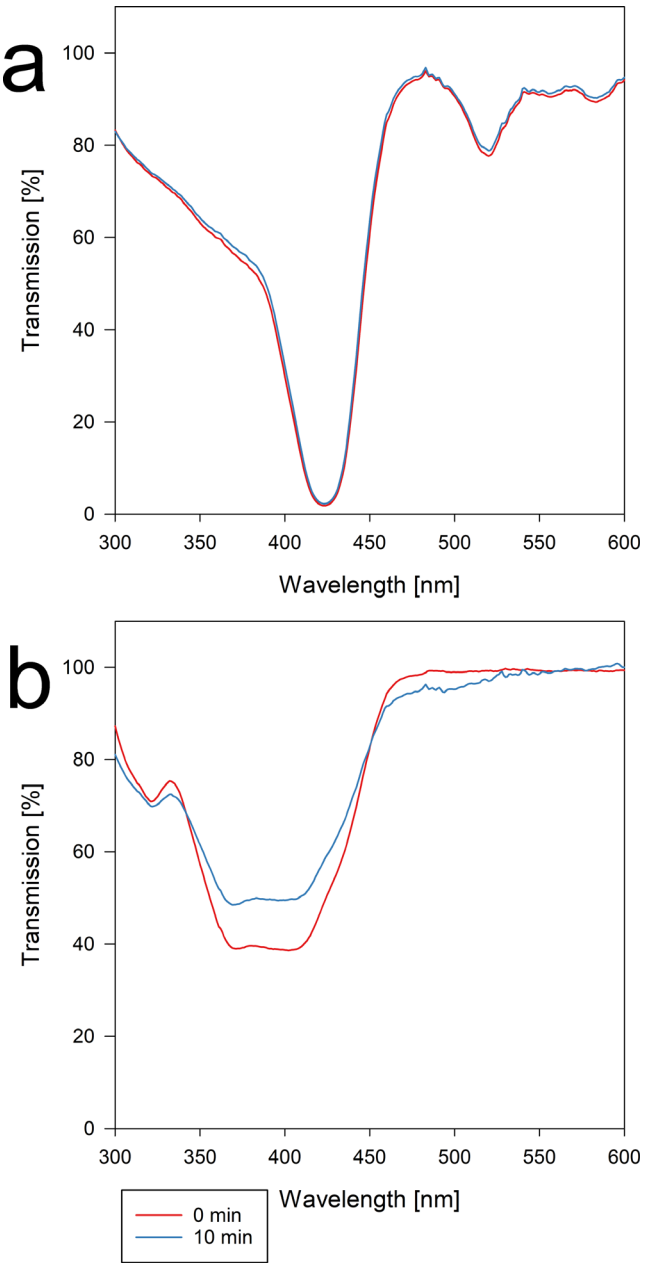

Figure 1. Transmission spectra for TMPyP (a) and SAPYR (b) dissolved in 10% (w/v) NaCl. Red lines refer to the nonilluminated control, while blue lines refer to photosensitizer solution after illumination at a radiant exposure of 10.8 J cm^{-2}.

$$\rho = \log 2^{\frac{\Delta t}{\Delta t_D}}$$

Attachment of photosensitizers to cells. In order to investigate the attachment of the photosensitizer to the cell surface, a culture grown as mentioned before was centrifuged at 4500 ***g*** for 7 min and final optical density at 600 nm was adjusted to 0.6. The supernatant was discarded and the cells were suspended in 500 µL of 10% (w/v) NaCl and 500 µL of 20 µmol L^{-1} of photosensitizer solution. Cells were mixed thoroughly and centrifuged again. The supernatant was measured in a photometer at a wavelength of 421 nm for TMPyP and 370 nm for SAPYR, resembling the corresponding absorption maxima. As blank, a 10% (w/v) NaCl solution was used. Control consisted of 5 µmol L^{-1} in a 10% (w/v) NaCl solution.

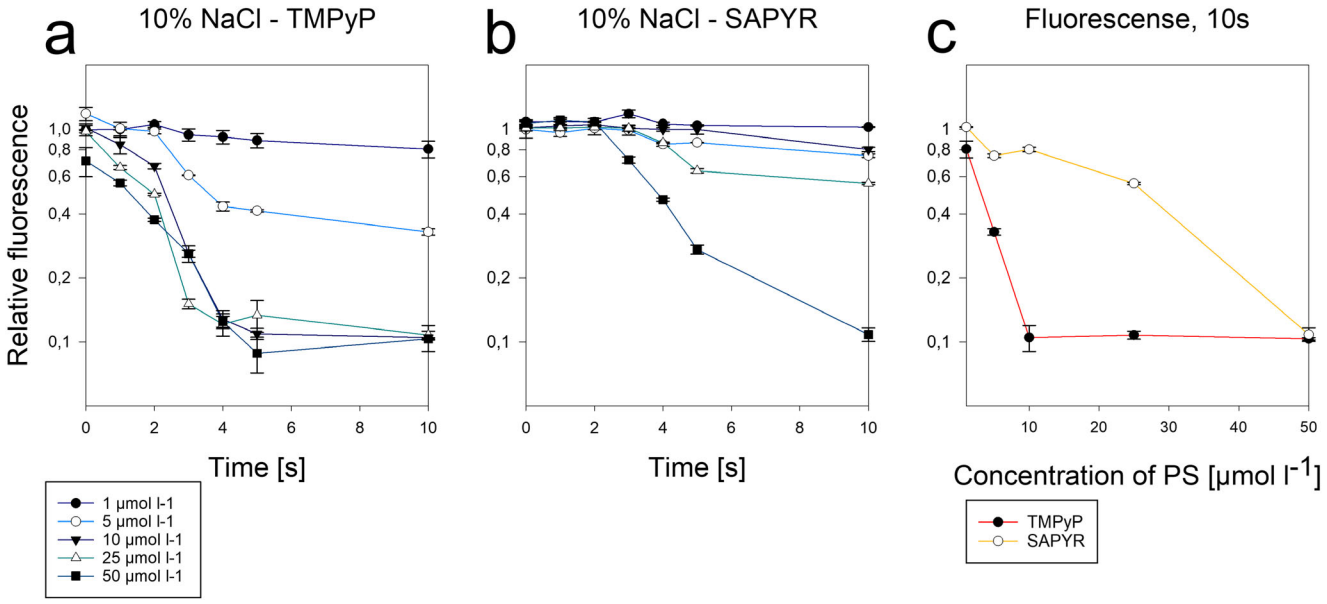

Figure 2. DPBF assays for TMPyP (a) and SAPYR (b) carried out in a 10% NaCl solution. Relative fluorescence is displayed logarithmically on the *y*-axis, and illumination time in seconds is plotted on *x*-axis. A comparison of the relative fluorescence (*y*-axis) for different photosensitizer concentrations (*x*-axis) is shown after 10 s of illumination equal to a total applied radiant exposure of 0.018 J cm^{-2} (c).

DPBF (1,3-Diphenylisobenzofuran) assays. For analyzing the production of singlet oxygen production under high salt concentrations, photosensitizer in final concentrations of 1, 5, 10, 25 and 50 μmol^{-1} and sodium chloride (20% w/v) were mixed and resuspended with the DPBF reagent with MeOH as a solvent to a total volume of 200 µL. Final concentrations were 1, 5, 10, 25 and 50 µmol L^{-1}, 500 µmol L^{-1} DPBF and 10% (w/v) NaCl. DPBF was excited in a spectral photometer (CLARIOStar, BMG LABTECH GmbH) at 411 nm while emission was detected at 451 nm. Relative fluorescence was calculated from a control without PS as $\frac{Fluorescence_{PS}}{Fluorescence_{Control}}$. Data were plotted *via* SigmaPlot V14. Control measurement was performed with a nonilluminated sample. The generation of singlet oxygen was then initiated *via* illumination beneath the light source blue_v applying a fluence of 0.018 J cm^{-2}, and fluorescence was measured as mentioned above. The illumination and measurements were repeated four times with the same sample. A final illumination with the same sample was performed applying another 0.09 J cm^{-2}. The applied fluence was equal to 1, 2, 3, 4, 5 and 10 s of illumination time in total.

Measurement of absorption spectra. Photosensitizer concentrations were prepared and mixed with an equal volume of 10% (w/v) NaCl solution in 96-well microreaction plates with a total volume of 100 µL. Spectra were recorded from 300 to 700 nm. Measurements took place with the illuminated and nonilluminated samples. The applied radiant exposure was 10.8 J cm^{-2} corresponding to 10 min of illumination.

RESULTS

Under high salt concentrations (10% [w/v] NaCl), no alterations of TMPyP absorption spectrum were detectable after irradiation (10.8 J cm^{-2}) (Fig. 1a). In contrast, SAPYR showed photobleaching after an applied radiant exposure of 10.8 J cm^{-2} (Fig. 1b). The data of the reference spectra with the photosensitizer dissolved in ultrapure water are not shown, as the curves did not differ from the nonirradiated sodium chloride controls.

Attachment assays showed that TMPyP binds much more efficient to the tested archaeal cells than SAPYR does. 73 % of TMPyP (3.62 µmol L^{-1}) attached to cells at a concentration of 5 µmol L^{-1}. In case of SAYPR, only 14 % (0.70 µmol L^{-1}) attached to the cells.

DPBF assays indicate that the production of singlet oxygen takes place with both dyes under high sodium chloride concentrations (Fig. 2). TMPyP generated more singlet oxygen when compared to SAPYR under the experimental conditions. For the highest concentration of 50 µmol L^{-1}, the same fluorescence is observed, indicating that either the same amount of oxygen was produced or all the available oxygen was depleted within the reaction. After 10 s of illumination, 50 µmol L^{-1} TMPyP (Fig. 2a) yielded a relative fluorescence of 10.3% and 11.0% for 50 µmol L^{-1} SAPYR (Fig. 2b), respectively. 25 µmol L^{-1} of photosensitizer showed a relative fluorescence of 10.2% for TMPyP and 55.6% for SAPYR, respectively. At 10 µmol L^{-1}, barely reduced relative fluorescence for TMPyP after 10 s was detected (10.5%) while SAPYR exhibited a tremendously higher relative fluorescence with 80.3%. 32.9% for 5 µmol L^{-1} TMPyP and 75.1% for 5 µmol L^{-1} SAPYR were the measured relative fluorescence values for mentioned concentration. 1 µmol L^{-1} of photosensitizer led to a relative fluorescence of 80.7% for TMPyP and 102.4% for SAPYR. Water controls after 10 s of illumination for SAPYR (data not shown) showed values of 22.6% for 50 µmol L^{-1}, 39.9% for 25 µmol L^{-1}, 64.2% for 10 µmol L^{-1}, 76.9% for 5 µmol L^{-1} and 107.4% for 1 µmol L^{-1}. Water controls for TMPyP showed after 10 s of illumination: 10.2% for 50 µmol L^{-1}, 10.3% for 25 µmol L^{-1}, 10.5% for 10 µmol L^{-1}, 16.5% for 5 µmol L^{-1} and 84.5% for 1 µmol L^{-1}. Fig. 2c compares the relative fluorescence for SAPYR and TMPyP after 10 s of illumination in dependence of the concentration of the photosensitizer.

The growth curves displayed in Fig. 3a clearly show that for the highest concentrations of SAPYR (25 and 50 µmol L^{-1}), no growth of *H. salinarum* was detected. Even after 4115 min of incubation, optical density values have not reached values above 0.1 (data not shown). The calculated $\log_{10}$ reductions for SAPYR are displayed in Fig. 3b. Significant $\log_{10}$ reductions were obtained for photosensitizer concentrations of 25 and 50 µmol L^{-1}.

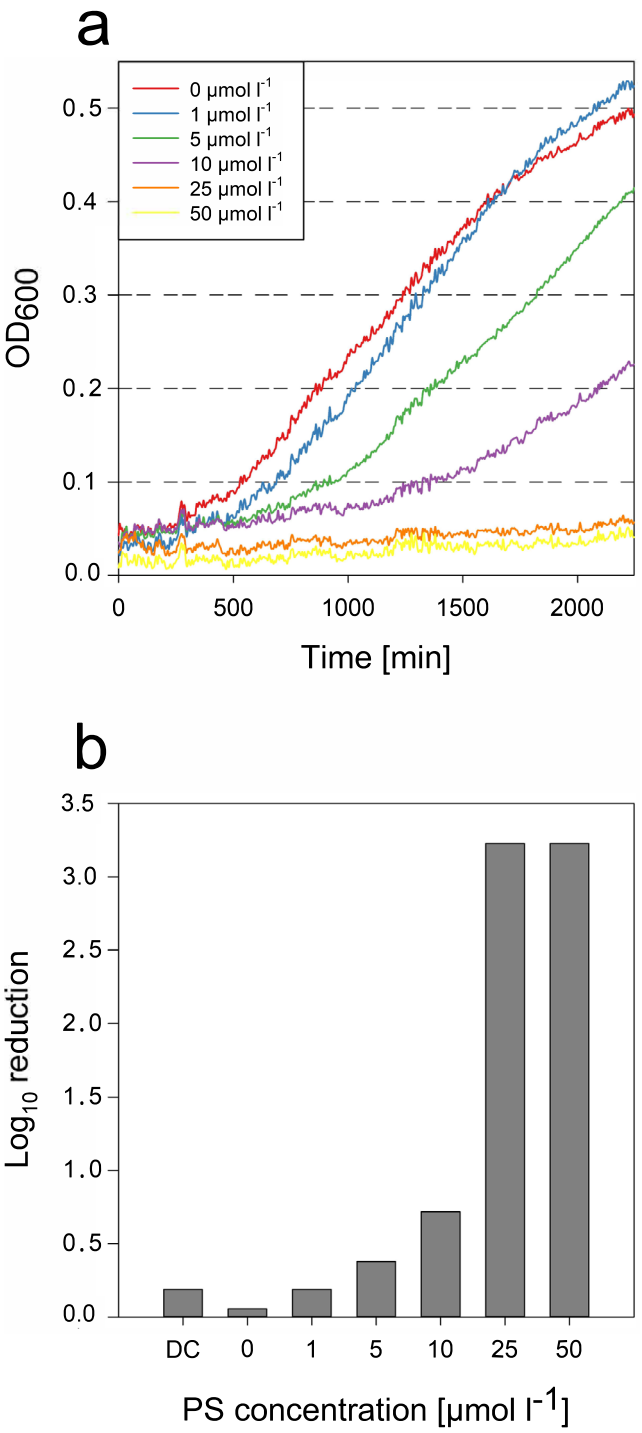

Figure 3. (a) Growth curves of *H. salinarum* after PDI treatment with SAPYR as photosensitizer. Different colors reflect the different SAPYR concentrations used for PDI treatment. *Y*-axis indicates the optical density measured at 600 nm. *X*-axis indicates the time in minutes. (b) Calculated $\log_{10}$ reduction displayed as bar chart diagram.

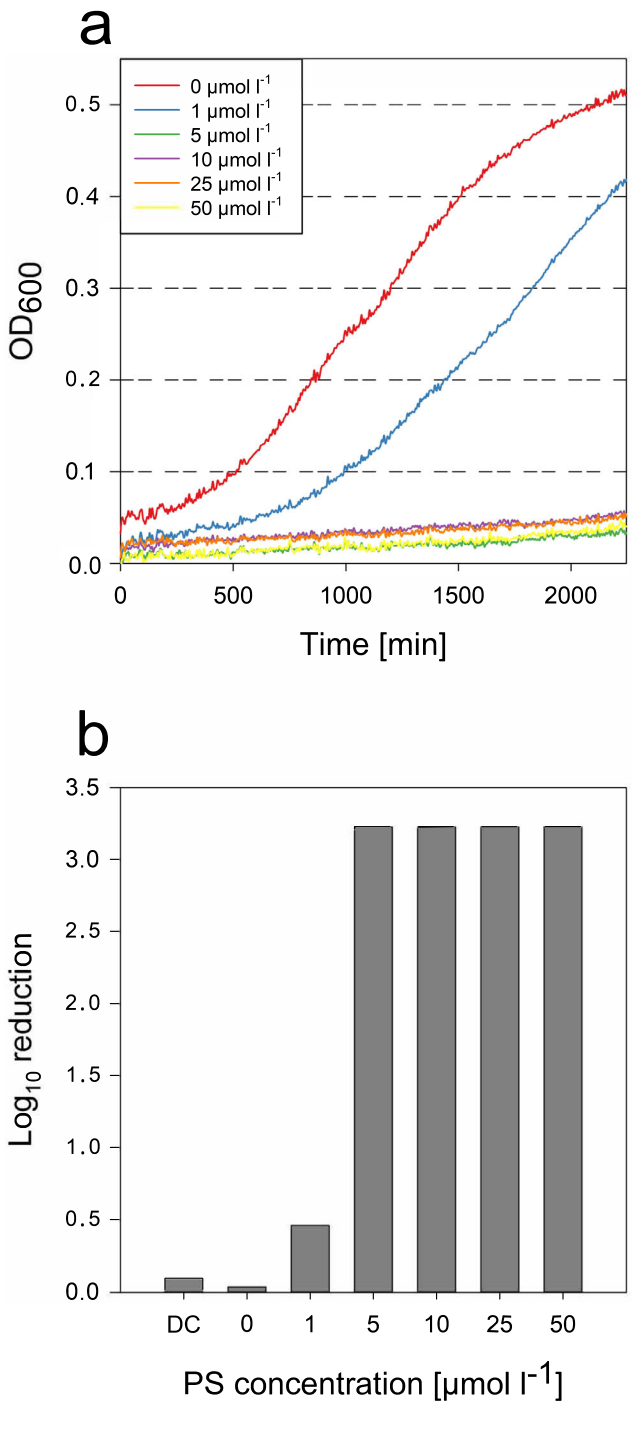

Figure 4. (a) Growth curves of *H. salinarum* after PDI treatment with TMPyP as Photosensitizer. Different colors reflect the different photosensitizer concentrations used for PDI treatment. *Y*-axis indicates the optical density measured at 600 nm. *X*-axis indicates the time in minutes. (b) Calculated $\log_{10}$ reduction displayed as bar chart diagram.

The illuminated control without photosensitizer exhibited a logarithmic reduction of 0.05.

When using the same concentrations of TMPyP and radiant exposure, the inactivation of *H. salinarum* was more efficient as shown by the growth curves in Fig. 4a compared to SAPYR (Fig. 3). The lowest photosensitizer concentration was 5 µmol L^{-1} to achieve maximal logarithmic reduction of 3.22. At 4115 min, TMPyP concentrations from 5 to 50 µmol L^{-1} showed that optical density did not exceed values above 0.1 resulting in a microbial reduction of at least 3 orders of magnitude. Dark control for TMPyP at 50 µmol L^{-1} showed no relevant logarithmic reduction with a calculated value of 0.09. The

logarithmic reduction values are displayed as a bar chart in Fig. 4b.

DISCUSSION

The presented results clearly show that the Archaeum *Halobacterium salinarum* can be efficiently inactivated (>99.9%) using PDI with either photosensitizer at low concentrations. The results also show that high concentrations of sodium chloride, for example, 10%, did not lead to a chemical alteration of the photosensitizers used. The loss of concentration after illumination for SAPYR is a general feature of the molecule, observed even in water without further substances present.

The structure of archaeal cells shows significant differences when compared to eukarya or bacteria. One of the most striking differences is their outer structure. Besides an S-Layer, which is also known for some bacteria, archaea are characterized by their extraordinary membrane structure. The phospholipid bilayer membrane consists of side chains of 20 carbon atoms built from isoprene attached with an ether linkage to glycerol compared to eukarya and bacteria that form ester bonds with fatty acids (35,36). Another obvious feature of halophilic archaea is the pink-to-purple color of the cells due to retinal bound to rhodopsin-like molecules named bacteriorhodopsin (37). Bacteriorhodopsin is an integral membrane protein with seven near-parallel alpha helices, whereas between the helices a retinal molecule is integrated as ligand forming a trimer composed of 21 helices and three retinal molecules (38). This protein functions as a light-driven proton pump contributing to the formation of a proton gradient for energy conservation (39). As rhodopsin and bacteriorhodopsin are structurally and chemically very similar, the singlet oxygen-quenching rate constant for rhodopsin should be quite similar to bacteriorhodopsin, at least within the same order of magnitude. The reported value for the quenching rate is 1.1×10^9 L mol^{-1} s^{-1}, therefore being similar to the ones found in literature for the azide ion (40–43). The presented results clearly show that archaeal structures compared to bacteria should have an impact on the efficiency but do not lead to a certain resistance or tolerance. Recently, van der Oost and coworkers engineered an *E. coli* cell capable of producing and incorporating archaeal lipids into the cell membranes (44). The impact of archaeal lipids concerning the susceptibility toward ROS could be studied in a sophisticated manner in future research utilizing the mentioned *E. coli* with the hybrid membrane.

This study also showed that archaeal structures like S-layer, rhodopsin or ether lipids did not prevent binding of the photosensitizer. It should be noted that the present investigation cannot differentiate whether photosensitizer molecules are taken up by the archaeal cells or are attached to the cellular wall only. The amounts of photosensitizer bound to the cells differ for both photosensitizers used. This difference might be explained by the different charges of the photosensitizers. SAPYR molecule exhibits only one positive charge while TMPyP four. Thus, TMPyP should attach much better to negatively charged outer structures of cells in general. As for bacterial cells, the S-layer of *Halobacterium* is negatively charged as the charge also maintains the lattice of the S-layer (45–47).

DPBF assays in general are sufficient to detect the generation of singlet oxygen. Our data suggest that under the experimental conditions, TMPyP produced more singlet oxygen than SAPYR. However, the different extinction coefficients along with emission spectrum of the light source and the photosensitizer concentrations must be considered. The impact of the absorbed photons on photosensitizers was thoroughly investigated elsewhere (48). According to that publication, the amounts of absorbed photons per second were compared. Additionally, the different singlet oxygen quantum yields were considered which are 0.77 for TMPyP (49) and 0.99 for SAPYR (50). Under present experimental conditions, SAPYR generates 94% or 62% less singlet oxygen than TMPyP for 1 or 50 μmol L^{-1} photosensitizer concentrations, respectively. These data should explain to some extent the difference in singlet oxygen production (DPBF assays; Fig. 2) and consequently also in PDI of *Halobacterium salinarum* for both photosensitizers (Figs. 3 and 4). Nevertheless, a reduction of viable cells is achieved for both photosensitizers with more than 3 $\log_{10}$ at 5 μmol L^{-1} (TMPyP) or 25 μmol L^{-1} (SAPYR). Our study showed that photodynamic inactivation of archaea works well and efficiently even at high salt concentrations. However, when compared to other model organisms like *E. coli*, *B. atrophaeus* or *E. faecalis*, *Halobacterium salinarum* seems to be less susceptible to PDI (33,48,50).

Various studies concerning photodynamic inactivation focus primarily on pathogenic bacteria causing severe skin infection (8,51–53). Nevertheless, the contribution of archaea to the human health in general is highly debated and highlighted (54–56). Up to date, there are no representatives known within the archaea that can cause pathogenic infections. However, it is known that archaea are able to colonize the human body (23,54,57–59). The role of *Methanobrevibacter oralis* in gingivitis and brain abscesses has been described (60,61).

When looking at the second goal of the present study, the data indicate that the presented method for high-throughput measurement of the antimicrobial potential can be applied to any microorganisms in liquid medium. The presented method offers several advantages compared to other methods like spread plating, pour plating or drop plating. First, the method offers huge time saving as the process of measuring and partly evaluation is automated. Compared to plating methods, a dilution series is not necessary, as well as plating is obviously not performed. Furthermore, the method is much cheaper than plating methods as no agar medium is necessary and the experiments can be performed within the microvolume range. Drop plating methods have some issues like accuracy and limitations to certain cells; however, the problems were mentioned and tried to optimize elsewhere (32).

CONCLUSIONS

The presented results are the first record for the photodynamic inactivation of archaea, therefore proving the applicability of PDI toward all domains of life. The novel method for generating high-throughput growth curves will prove useful in the future concerning research of antimicrobial substances in general, as the method is applicable for all organisms that grow in liquid media. Our future research concerning photodynamic inactivation of archaea will focus on the role of archaeal lipids concerning photodynamic inactivation.

Acknowledgements—Technical help of G. Gmeinwieser is highly appreciated. This work was supported by the German Research Foundation DFG [grant number 415812443].

REFERENCES

1. Raab, O. (1900) Über die Wirkung fluorescierender Stoffe auf Infusorien. *Z. Biol.* **39**, 524–546.
2. von Tappeiner, H. and A. Jodlbauer (1904) Über die Wirkung der photodynamischen (fluorescierenden) Stoffe auf Protozoen und Enzyme. *Arch. Klin. Med.* **80**, 427–487.
3. von Tappeiner, H. (1900) Über die Wirkung fluorescierender Stoffe auf Infusorien nach Versuchen von Raab. *Münch. Med. Wochenschr.* **1**, 5–7.
4. Robertson, C. A., D. H. Evans and H. Abrahamse (2009) Photodynamic therapy (PDT): A short review on cellular mechanisms and cancer research applications for PDT. *J. Photochem. Photobiol. B Biol.* **96**, 1–8.
5. Wainwright, M., T. Maisch, S. Nonell, K. Plaetzer, A. Almeida, G. P. Tegos and M. R. Hamblin (2017) Photoantimicrobials – Are we afraid of the light? *Lancet Infect. Dis.* **17**, e49–e55.
6. Yin, R. and M. R. Hamblin (2015) Antimicrobial photosensitizers: Drug discovery under the spotlight. *Curr. Med. Chem.* **22**, 2159–2185.
7. Maisch, T., A. Eichner, A. Späth, A. Gollmer, B. König, J. Regensburger and W. Bäumler (2014) Fast and effective photodynamic inactivation of multiresistant bacteria by cationic riboflavin derivatives. *PLoS One* **9**, e111792.
8. Späth, A., W. Bäumler, D. Eckl, M. Schreiner, A. Eichner and B. König (2018) MRSA decolonization of human skin via photodynamic treatment. *Br. J. Dermatol.* **179**, e242–e242.
9. Eichner, A., T. Holzmann, D. B. Eckl, F. Zeman, M. Koller, M. Huber, S. Pemmerl, W. Schneider-Barchert and W. Bäumler (2019) Novel photodynamic coatings reduce the bioburden on near-patient surface thereby reducing the risk for onward pathogen transmission – a field study in two hospitals. *J. Hosp. Infect.* **104**(1), 85–91. in press. https://doi.org/10.1016/j.jhin.2019.07.016
10. Rywkin, S., L. Lenny, J. Goldstein, N. E. Geacintov, H. Margolis-Nunno and B. Horowitz (1992) Importance of type I and type II mechanisms in the photodynamic inactivation of viruses in blood with aluminium phthalocyanine derivates. *Photochem. Photobiol.* **56**, 463–469.
11. Lenard, J. and R. Vanderoef (1993) Photoinactivation of influenza virus fusion and infectivity bay rose bengal. *Photochem. Photobiol.* **58**, 527–531.
12. Degar, S., A. M. Prince, D. Pascual, G. Lavie, B. Levin, Y. Mazur, D. Lavie, L. S. Ehrlich, C. Carter and D. Meruelo (2009) Inactivation of the human immunodeficiency virus by hypericin: Evidence for photochemical alterations of p24 and a block in uncoating. *AIDS Res. Hum. Retroviruses* **8**, 1929–1936.
13. Egyeki, M., G. Turóczy, Z. Majer, K. Tóth, A. Fekete, P. Maillard and G. Csík (2003) Photosensitized inactivation of T7 phage as surrogate of non-enveloped DNA viruses: Efficiency and mechanism of action. *Biochim. Biophys. Acta Gen. Subj.* **1624**, 115–124.
14. Gábor, F., J. Szolnoki, K. Tóth, A. Fekete, P. Maillard and G. Csík (2004) Photoinduced inactivation of T7 phage sensitized by symmetrically and asymmetrically substituted tetraphenyl porphyrin: comparison of efficiency and mechanism of action. *Photochem. Photobiol.* **73**, 304.
15. Badireddy, A. R., E. M. Hotze, S. Chellam, P. Alvarez and M. R. Wiesner (2007) Inactivation of bacteriophages via photosensitization of fullerol nanoparticles. *Environ. Sci. Technol.* **41**, 6627–6632.
16. Pereira Gonzales, F. and T. Maisch (2012) Photodynamic inactivation for controlling *Candida albicans* infections. *Fungal Biol.* **116**, 1–10.
17. Quiroga, E. D., M. G. Alvarez and E. N. Durantini (2010) Susceptibility of *Candida albicans* to photodynamic action of 5,10,15,20-tetra(4-N-methylpyridyl)porphyrin in different media. *FEMS Immunol. Med. Microbiol.* **60**, 123–131.
18. Eichner, A., F. P. Gonzales, A. Felgenträger, J. Regensburger, T. Holzmann, W. Schneider-Brachert, W. Bäumler and T. Maisch (2013) Dirty hands: photodynamic killing of human pathogens like EHEC, MRSA and *Candida* within seconds. *Photochem. Photobiol. Sci.* **12**, 135–147.
19. Gonzales, F. P., S. H. Da Silva, D. W. Roberts and G. U. L. Braga (2010) Photodynamic inactivation of conidia of the fungi *Metarhizium anisopliae* and *Aspergillus nidulans* with methylene blue and toluidine blue. *Photochem. Photobiol.* **86**, 653–661.
20. Soares, B. M., O. A. Alves, M. V. L. Ferreira, J. C. F. Amorim, G. R. Sousa, L. de Barros Silveira, R. A. Prates, T. V. Ávila, L. de Matos Baltazar, D. da Glória de Souza, D. A. Santos, L. V. Modolo, P. S. Cisalpino and M. Pinotti (2011) *Cryptococcus gattii*: *In vitro* susceptibility to photodynamic inactivation. *Photochem. Photobiol.* **87**, 357–364.
21. Gardlo, K., Z. Horska, C. D. Enk, L. Rauch, M. Megahed, T. Ruzicka and C. Fritsch (2003) Treatment of cutaneous leishmaniasis by photodynamic therapy. *J. Am. Acad. Dermatol.* **48**, 893–896.
22. Horz, H. P. (2015) Archaeal lineages within the human microbiome: Absent, rare or elusive? *Life* **5**, 1333–1345.
23. Probst, A. J., A. K. Auerbach and C. Moissl-Eichinger (2013) Archaea on human skin. *PLoS One* **8**, e65388.
24. Dridi, B., D. Raoult and M. Drancourt (2011) Archaea as emerging organisms in complex human microbiomes. *Anaerobe* **17**, 56–63.
25. Jolivet, E., S. L'Haridon, E. Corre, P. Forterre and D. Prieur (2003) *Thermococcus gammatolerans* sp. nov., a hyperthermophilic archeon from a deep-sea hydrothermal vent that resists ionizing radiation. *Int. J. Syst. Evol. Microbiol.* **53**, 847–851.
26. Schleper, C., G. Pühler, H. P. Klenk and W. Zillig (1996) *Picrophilus oshimae* and *Picrophilus torridus* fam. nov., gen. nov., sp. nov., two species of hyperacidophilic, thermophilic, heterotrophic, aerobic archaea. *Int. J. Syst. Bacteriol.* **46**, 814–816.
27. Mora, M., L. Wink, I. Kögler, A. Mahnert, P. Rettberg, P. Schwendner, R. Demets, C. Cockell, T. Alekhova, A. Klingl, R. Krause, A. Zolotariof, A. Alexandrova and C. Moissl-Eichinger (2019) Space station conditions are selective but do not alter microbial characteristics relevant to human health. *Nat. Commun.* **10**, 3990.
28. Ranck, R. O. (1957) *Some Reactions of Phenothiazine and its Derivatives*. Iowa State College, Ames, Iowa.
29. Harrison, F. C. and M. E. Kennedy (1922) The red discolouration of cured codfish. *Proc. R. Soc. Canada* **5**, 101–152.
30. Elazari-Volcani, B. (1957) *Bergey's Manual of Determinative Bacteriology Genus XII Halobacterium*. (Edited by Murray and Smith). Williams & Wilkins, Baltimore, Maryland.
31. Miles, A. A., S. S. Misra and J. O. Irwin (1938) The estimation of the bactericidal power of the blood. *J. Hyg. (Lond)* **38**, 732–749.
32. Herigstad, B., M. Hamilton and J. Heersink (2001) How to optimize the drop plate method for enumerating bacteria. *J. Microbiol. Methods* **44**, 121–129.
33. Eckl, D. B., L. Dengler, M. Nemmert, A. Eichner, W. Bäumler and H. Huber (2018) A closer look at dark toxicity of the photosensitizer TMPyP in bacteria. *Photochem. Photobiol.* **94**, 165–172.
34. Bechert, T., P. Steinrücke and J. P. Guggenbichler (2000) A new method for screening anti-infective biomaterials. *Nat. Med.* **6**, 1053–1056.
35. Upasani, V. N., S. G. Desai, N. Moldoveanu and M. Kates (1994) Lipids of extremely halophilic archaeobacteria from saline environments in India: A novel glycolipid in *Natronobacterium* strains. *Microbiology* **140**, 1959–1966.
36. Kate, M. (1993) Membrane lipids of archaea. *New Compr. Biochem.* **26**, 261–295.
37. Oesterhelt, D. and W. Stoeckenius (1971) Rhodopsin-like protein from the purple membrane of *Halobacterium halobium*. *Nat. New Biol.* **233**, 149–152.
38. Schobert, B., J. Cupp-Vickery, V. Hornak, S. O. Smith and J. K. Lanyi (2002) Crystallographic structure of the K intermediate of bacteriorhodopsin: Conservation of free energy after photoisomerization of the retinal. *J. Mol. Biol.* **321**, 715–726.
39. Oesterhelt, D. and W. Stoeckenius (1973) Functions of a new photoreceptor membrane. *Proc. Natl Acad. Sci. USA* **70**, 2853–2857.
40. Rubio, M. A., D. O. Mártire, S. E. Braslavsky and E. A. Lissi (1992) Influence of the ionic strength on O2(1□g) quenching by azide. *J. Photochem. Photobiol. A Chem.* **66**, 153–157.
41. Starostin, A. V., I. B. Fedorovich and M. A. Ostrovskii (1988) Photooxidation of rhodopsin. Oxygen consumption and action spectrum. *Biofizika* **33**, 452–455.
42. Krasnovsky, A. A. and V. E. Kagan (1979) Photosensitization and quenching of singlet oxygen by pigments and lipids of photoreceptor cells of the retina. *FEBS Lett.* **108**, 152–154.
43. Wilkinson, F., W. P. Helman and A. B. Ross (1995) Rate constants for the decay and reactions of the lowest electronically excited singlet state of molecular oxygen in solution. An expanded and revised compilation. *J. Phys. Chem. Ref. Data* **24**, 663–677.

44. Caforio, A., M. F. Siliakus, M. Exterkate, S. Jain, V. R. Jumde, R. L. H. Andringa, S. W. M. Kengen, A. J. Minnaard, A. J. M. Driessen and J. van der Oost (2018) Converting *Escherichia coli* into an archaebacterium with a hybrid heterochiral membrane. *Proc. Natl Acad. Sci. USA* **115**, 3704–3709.
45. Sumper, M. (1993) S-layer glycoproteins from moderately and extremely halophilic archaeobacteria. In *Advances in Bacterial Paracrystalline Surface Layers*, pp. 109–117. (Edited by T.J. Beveridge and S.F. Koval). Springer, Boston, Massachusetts.
46. Sleytr, U. B., D. Pum, E. M. Egelseer, N. Ilk and B. Schuster (2013) S-layer proteins. *Handbook of Biofunctional Surfaces*, pp. 507–568. (Edited by Wolfgang Knoll). Jenny Stanford Publishing, Singapore.
47. Mescher, M. F. and J. L. Strominger (1976) Purification and characterization of a prokaryotic glycoprotein from the cell envelope of *Halobacterium salinarium*. *J. Biol. Chem.* **251**, 2005–2014.
48. Cieplik, F., A. Pummer, J. Regensburger, K. A. Hiller, A. Späth, L. Tabenski, W. Buchalla and T. Maisch (2015) The impact of absorbed photons on antimicrobial photodynamic efficacy. *Front. Microbiol.* **6**, 706. https://doi.org/10.3389/fmicb.2015.00706
49. Baier, J., T. Maisch, J. Regensburger, M. Loibl, R. Vasold and W. Bäumler (2007) Time dependence of singlet oxygen luminescence provides an indication of oxygen concentration during oxygen consumption. *J. Biomed. Opt.* **12**, 64008.
50. Cieplik, F., A. Späth, J. Regensburger, A. Gollmer, L. Tabenski, K. A. Hiller, W. Bäumler, T. Maisch and G. Schmalz (2013) Photodynamic biofilm inactivation by SAPYR – An exclusive singlet oxygen photosensitizer. *Free Radic. Biol. Med.* **65**, 477–487.
51. Tang, H. M., M. R. Hamblin and C. M. N. Yow (2007) A comparative *in vitro* photoinactivation study of clinical isolates of multidrug-resistant pathogens. *J. Infect. Chemother.* **13**, 87–91.
52. Pérez-Laguna, V., L. Pérez-Artiaga, V. Lampaya-Pérez, I. García-Luque, S. Ballesta, S. Nonell, M. P. Paz-Cristobal, Y. Gilaberte and A. Rezusta (2017) Bactericidal effect of photodynamic therapy, alone or in combination with mupirocin or linezolid, on *Staphylococcus aureus*. *Front. Microbiol.* **8**, 1002. https://doi.org/10.3389/fmicb.2017.01002
53. Späth, A., A. Graeler, T. Maisch and K. Plaetzer (2018) CureCuma–cationic curcuminoids with improved properties and enhanced antimicrobial photodynamic activity. *Eur. J. Med. Chem.* **159**, 423–440.
54. Koskinen, K., M. R. Pausan, A. K. Perras, M. Beck, C. Bang, M. Mora, A. Schilhabel, R. Schmitz and C. Moissl-Eichinger (2017) First insights into the diverse human archaeome: Specific detection of Archaea in the gastrointestinal tract, lung, and nose and on skin. *MBio* **8**, e00824–17.
55. Nkamga, V. D., B. Henrissat and M. Drancourt (2017) Archaea: Essential inhabitants of the human digestive microbiota. *Hum. Microbiome J.* **3**, 1–8.
56. Lurie-Weinberger, M. N. and U. Gophna (2015) Archaea in and on the human body: Health implications and future directions. *PLoS Pathog.* **11**, e1004833.
57. Miller, T. L., M. J. Wolin, E. C. De Macario and A. J. L. Macario (1982) Isolation of *Methanobrevibacter smithii* from human feces. *Appl. Environ. Microbiol.* **43**, 227–232.
58. Belay, N., R. Johnson, B. S. Rajagopal, E. C. De Macario and L. Daniels (1988) Methanogenic bacteria from human dental plaque. *Appl. Environ. Microbiol.* **54**, 600–603.
59. Belay, N., B. Mukhopadhyay, E. Conway de Macario, R. Galask and L. Daniels (1990) Methanogenic bacteria in human vaginal samples. *J. Clin. Microbiol.* **28**, 1666–1668.
60. Ferrari, A., T. Brusa, A. Rutili, E. Canzi and B. Biavati (1994) Isolation and characterization of *Methanobrevibacter oralis* sp. nov. *Curr. Microbiol.* **29**, 7–12.
61. Drancourt, M., V. D. Nkamga, N. A. Lakhe, J. M. Régis, H. Dufour, P. E. Fournier, Y. Bechah, W. Michael Scheld and Di Raoult (2017) Evidence of archaeal methanogens in brain abscess. *Clin. Infect. Dis.* **65**, 1–5.